JGR Atmospheres

RESEARCH ARTICLE
10.1029/2024JD042899

Future Local-Scale Extreme Precipitation Changes in Norway: A Convection-Permitting Climate Model Perspective

Kun Xie[1], Lu Li[2], Hua Chen[1], Stephanie Mayer[2], Stefan P. Sobolowski[3], and Chong-Yu Xu[4]

[1]School of Water Resources and Hydropower Engineering, Wuhan University, Wuhan, P. R. China, [2]NORCE Norwegian Research Centre, and Bjerknes Centre for Climate Research, Bergen, Norway, [3]Geophysical Institute, University of Bergen and the Bjerknes Center for Climate Research, Bergen, Norway, [4]Department of Geosciences, University of Oslo, Oslo, Norway

Abstract Building on previous work demonstrating the skill of high-resolution Convection-Permitting Regional Climate Models in simulating extreme precipitation at local to regional scales, this study explores future projections of hourly and daily extreme precipitation across Norway. We use data from the HARMONIE-Climate (HCLIM) model applied at 12 and 3 km resolutions and examine the extreme precipitation response by the middle and end of the century in the RCP8.5 emission scenario. Our results show that: (a) precipitation intensity is projected to increase across almost all regions, except for daily extremes from HCLIM models driven by EC-EARTH global climate model (GCM) in the southern and south-western regions. HCLIM simulations driven by GFDL-CM3 GCM project a larger increase in extremes compared with those driven by EC-EARTH, which is likely associated with the stronger warming and moistening seen in GFDL-CM3 over northern Europe in this scenario. (b) Frequency of both hourly and daily extremes is projected to increase in the future. However, the seasonality of extremes does not exhibit a shift, except for hourly extremes in the western region shifting from autumn-winter to spring-summer, and southern region shifting from spring-summer to autumn-winter. (c) Convection-permitting simulations (∼3 km grid spacing) show a larger increase in extreme precipitation at both daily and hourly timescales across most seasons except winter while also projecting a comparable increase in the frequency of extreme events to convection-parameterized models (∼12 km) in most regions. This study highlights the critical role of high-resolution modeling in credibly capturing the local-scale spatiotemporal changes in extreme precipitation.

Plain Language Summary This study examines how extreme precipitation events in Norway could change in the future, focusing on both hourly and daily time scale. Using HCLIM regional climate models applied at 3 and 12 km horizontal resolutions, we investigate the change in precipitation intensity and frequency by the end of the 21st century. Our findings show that most regions of Norway are likely to experience more intense and frequent precipitation, particularly for hourly extremes. Simulations driven by GFDL-CM3 GCM shows a larger increase in extremes than those driven by EC-EARTH GCM with weaker warming and smaller increase in moisture. The seasonality of extreme precipitation in these models demonstrate no shift in most regions, except the southern and western regions. Notably, the high-resolution convection-permitting model projects a larger increase in extreme intensity but comparable increase in hourly and daily extreme event frequency than its coarser-resolution counterpart across most regions. This study highlights the need for high-resolution climate models to better understand how extreme precipitation might affect specific regions and locations in a warming world. Understanding these local changes is crucial to preparing for potential floods and managing water resources effectively.

Key Points:

- Future extreme precipitation changes over Norway are compared between the convection-permitting model HCLIM3 and the coarser model HCLIM12
- In most regions, hourly and daily extreme intensity and frequency are projected to increase, with no shift in seasonality
- HCLIM3 projects a larger increase of future extremes than HCLIM12 in most seasons and regions

Supporting Information:

Supporting Information may be found in the online version of this article.

Correspondence to:

H. Chen and L. Li,
chua@whu.edu.cn;
luli@norceresearch.no

Citation:

Xie, K., Li, L., Chen, H., Mayer, S., Sobolowski, S. P., & Xu, C.-Y. (2025). Future local-scale extreme precipitation changes in Norway: A convection-permitting climate model perspective. *Journal of Geophysical Research: Atmospheres*, *130*, e2024JD042899. https://doi.org/10.1029/2024JD042899

Received 13 NOV 2024
Accepted 26 JUN 2025

Author Contributions:

Conceptualization: Kun Xie, Lu Li
Formal analysis: Kun Xie
Funding acquisition: Stefan P. Sobolowski
Investigation: Kun Xie, Lu Li
Methodology: Kun Xie, Lu Li, Stephanie Mayer
Project administration: Stefan P. Sobolowski
Supervision: Lu Li, Hua Chen
Validation: Kun Xie
Visualization: Kun Xie
Writing – original draft: Kun Xie

1. Introduction

Continued warming will lead to an increase in extreme precipitation over Europe, causing a greater risk for subsequent flooding events (Tarasova et al., 2023). The 6th Assessment Report of the Intergovernmental Panel on Climate Change (IPCC AR6), expresses high confidence that extreme precipitation will increase in northern Europe. However, it remains a major challenge to simulate and project changes in extreme precipitation at regional or local scales using coarse-resolution GCM, which often fail to capture local-scale processes and are not able to realistically represent certain surface characteristics such as complex and steep topography (Kendon

Writing – review & editing: Kun Xie, Lu Li, Hua Chen, Stephanie Mayer, Stefan P. Sobolowski, Chong-Yu Xu

et al., 2023). Understanding these future changes is critical for risk and vulnerability assessments related to extreme precipitation and flooding. High-resolution spatiotemporal climate information has great potential for reliably projecting future changes in extreme precipitation. GCMs with grid spacing on the order of 100 km exhibit substantial uncertainty and model deficiencies in their representation of precipitation extremes (Chen et al., 2021; Kendon et al., 2019; Prein et al., 2015). This is not only because the models are too coarse to capture local features but also because these models rely heavily on parameterization schemes to represent convection (Kendon et al., 2023). Models with higher resolution, between 10 and 50 km resolution, may improve representation of regional scale features but are still reliant upon convective parameterization schemes, which struggle to represent daily to subdaily precipitation extremes (Fosser et al., 2020, 2024).

Convection-permitting regional climate models (CPRCMs) with grid-spacing of less than 4 km, obviate the necessity for parameterizations of atmospheric deep convection, and thus represent a promising alternative (Lucas-Picher et al., 2021). Fosser et al. (2024) and Kendon et al. (2017) demonstrated that CPRCMs offer greater confidence in climate projections for sub-daily and daily precipitation extremes compared with RCMs. In comparison to the drizzle phenomenon (characterized by high frequency but low-intensity precipitation) in models using convection parameterizations (Chen et al., 2021; Lind et al., 2022), CPRCMs have shown skill in modeling the intermittent and intense nature of extreme precipitation events (Chen et al., 2021). The projected pattern of change in extreme precipitation may differ markedly between CPRCMs and RCMs at hourly to daily scales, and the change may even have opposite sign in some locations (Chan et al., 2014; Fosser et al., 2020; Pichelli et al., 2021). For example, Chan et al. (2014) showed that CPRCMs projected an increase in hourly events for various return periods during summer over the southern UK, whereas RCMs indicated a decline in such occurrences. Pichelli et al. (2021) demonstrated a reversal in change of precipitation intensity when comparing RCMs and CPRCMs. Unrealistically large changes in precipitation extremes have also been seen in RCMs (Chapman et al., 2023). Regarding seasonality, most studies have indicated that CPRCMs project a greater intensification of sub-daily to daily precipitation extremes in summer (Chan et al., 2018; Fosser et al., 2020; Knist et al., 2020). However, the change patterns of extreme precipitation in winter are more consistent between RCMs and CPRCMs than in summer. For instance, Chan et al. (2018) and Knist et al. (2020) observed that both CPRCMs and RCMs exhibited comparable projections regarding the change of winter extreme precipitation. Furthermore, Vanden Broucke et al. (2019) demonstrated that the discrepancy between CPRCMs and RCMs in projecting future extreme precipitation is influenced by topography. They showed that CPRCMs predict a significant increase in extreme precipitation in both mountain and lowland areas while RCMs show a comparable increase in mountain areas but significantly underestimate the increase in extremes in lowlands. It is therefore recommended that a comparative analysis of the similarities and differences between CPRCM and RCM in future extreme precipitation projections from hourly to daily scales should be conducted at the regional or local level, with due consideration of seasonality.

Extreme precipitation at different temporal scales is closely associated with various weather systems (Kendon et al., 2023; Lavers et al., 2012), and shows varied response to climate change and inconsistency between different regions, particularly in Norway. Differential changes in sub-daily versus daily scale precipitation extremes is of much interest yet scarcely compared. Some studies have attempted to quantify the local temperature scaling of precipitation extremes to compare the response of sub-daily and daily extremes to climate warming in Europe (Hodnebrog et al., 2019; Knist et al., 2020; Utsumi et al., 2011), however, fail to account for other factors such as seasonal cycles of precipitation and topography (Vanden Broucke et al., 2019). Coarse resolution models often fail to capture these sub-daily extremes effectively (Hanel & Buishand, 2010), underscoring the need for detailed studies using high-resolution CPRCMs to assess the response of local extreme precipitation to warming. It is particularly important for regions with complex topography, such as Norway. Such extreme events drive severe hazards such as floods, avalanches, and landslides in Norway (Huo et al., 2022; Poujol et al., 2021). Building on previous work, Médus et al. (2022) and Xie et al. (2025) demonstrated the skill of CPRCMs in simulating historical extreme precipitation at local and regional scales. Future changes in hourly and daily precipitation intensity for both CPRCMs and RCMs have also been projected at large scales in the Fenno-Scandinavia and Nordic-Baltic regions by Lind et al. (2022) and Dyrrdal et al. (2023), respectively. This study aims to advance our understanding of the changing nature of extreme precipitation over Norway in a warming climate. Our objectives are: (a) to evaluate future changes in the daily and hourly extreme precipitation (including intensity, frequency, and seasonality); and (b) to conduct a comparison between CPRCMs and traditional RCMs to investigate their differences in precipitation extremes at regional to local scale precipitation extremes in Norway.

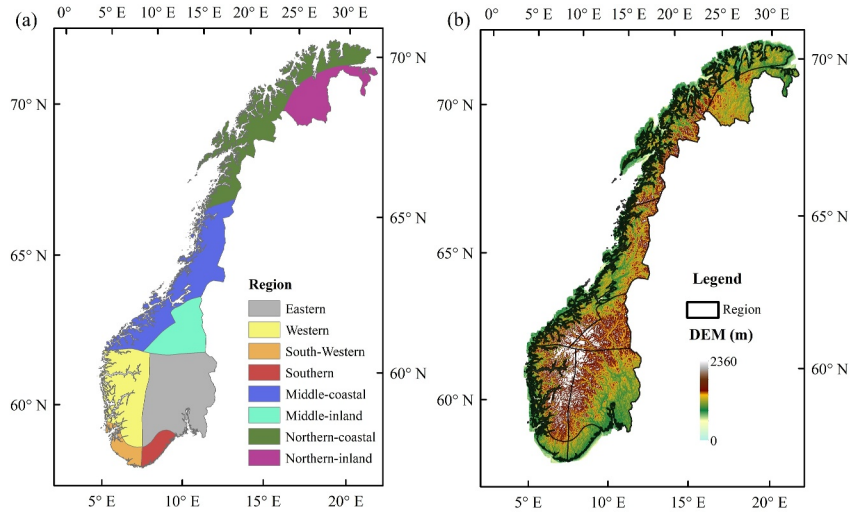

Figure 1. (a) The division of 8 precipitation regions in Norway; (b) topography of Norway.

2. Methods

In accordance with the characteristics of seasonal cycle and climate classifications (Konstali & Sorteberg, 2022; Michel et al., 2021), the Norwegian mainland was divided into eight regions, including Eastern (E), Southern (S), South-Western (SW), Western (W), Middle-Inland (MI), Middle-Coastal (MCo), Northern-Coastal (NCo), and Northern-Inland (NI) (Figure 1a). The topography for the Norwegian mainland is shown in Figure 1b. It is essential to analyze the CPRCMs projections at the sub-regional level for targeted flood and drought policy planning.

Our results are based on the output of double nested model simulations with the HARMONIE-Climate (HCLIM) regional climate model, cycle 38 (HCLIM38). Two GCMs (i.e., EC-EARTH and GFDL-CM3) under Representative Concentration Pathway (RCP) emissions scenarios RCP8.5 in the control period (CTRL: 1986–2005), the mid-century (MC: 2041–2060), and the end-century (LC: 2081–2100) periods are dynamically downscaled with HCLIM38 using two model configurations: (a) HCLIM38-ALADIN is run over a domain covering most of Europe, comprising 313 × 349 grid points at a grid spacing of 12 km (hereafter HCLIM12). EC-EARTH and GFDL-CM3 (GFDL) global climate models with grid spacing of 1.125° × 1.125° and 2.0° × 2.5°, respectively, provide the boundary conditions to HCLIM12. (b) HCLIM38-AROME is run over a domain covering the Fenno-Scandinavia region, comprising 637 × 853 horizontal grid points at a grid spacing of 3 km (hereafter HCLIM3). HCLIM12-E and HCLIM12-G refer to HCLIM12 simulations driven by EC-EARTH and GFDL, respectively, while HCLIM3-E and HCLIM3-G refer to the HCLIM3 simulations driven by EC-EARTH and GFDL, respectively. The convection parameterization scheme was switched-off in HCLIM3, thereby facilitating an explicit representation of convection processes. From 1980–2005 to 2071–2100, the GFDL model simulates a temperature increase of approximately 5.5°C and an increase in precipitation of 0.5 mm per day, which is higher than the EC-EARTH model that simulates an increase of 4°C and 0.2 mm per day, respectively. For a more comprehensive information of the modeling system and schemes, refer to the work of Lind et al. (2020, 2022). Xie et al. (2025) also conducted an evaluation of the performance of HCLIM3 and HCLIM12 in simulating extreme precipitation in the current period (1999–2018), and revealed that HCLIM3 provides a closer match to observational data than HCLIM12 for daily and hourly extreme precipitation (including maxima, frequency, and seasonality) in Norway. In contrast, HCLIM12 tends to underestimate extremes, with a more pronounced bias for hourly extremes. At the regional scale, HCLIM3 demonstrates superior accuracy in capturing the maximum 1-day precipitation (Rx1d) and maximum 1-hr precipitation (Rx1h) across most regions and seasons.

This study primarily focused on analyzing and comparing future changes in extreme precipitation from hourly to daily scales, at regional scales. We present projections from HCLIM3 and HCLIM12 forced by EC-EARTH and GFDL GCMs across eight regions of the Norwegian mainland. Prior to analysis, the data from HCLIM3 were regridded to the HCLIM12 grid (12 km). Precipitation intensity, Climate Factor (CF), frequency, and seasonality indices are calculated for both hourly and daily timescales. The indices were calculated at the grid-point level, and

then regional averages were taken. *T*-test (Efron, 1969) at a 5% significance level, with a critical value of 2.024, was employed to assess the statistical significance of the changes for the future annual maximum (AM) 1-day precipitation (Rx1d) and 1-hr precipitation (Rx1h) compared with the CTRL under the assumption that the extreme precipitation is normally distributed.

The Climate Factor (CF), as a standard climate adaptation indicator used in the climate factsheet of Norway (local municipalities), was employed to show the future change of extreme precipitation (Dyrrdal et al., 2023) and provides additional insights beyond a simple increase or decrease. Here, a CF was used to represent the future change of precipitation, which was defined as:

$$\mathrm{CF} = \frac{P_{\mathrm{fut}}}{P_{\mathrm{CTRL}}}, \tag{1}$$

Here, P_{CTRL} and P_{fut} represent the Rx1d/Rx1h in the CTRL and future time periods, respectively. If CF > 1, it meant that precipitation will increase in the future compared with CTRL. If CF < 1, it meant that precipitation will decrease in the future compared with CTRL.

The seasonality index S_D (Vormoor et al., 2015) was calculated for the CTRL, MC, and LC periods to explore the potential seasonal change of extreme precipitation, based on:

$$S_D = \frac{\mathrm{AM}_{\mathrm{Autumn-Winter}}}{\mathrm{AM}_{\mathrm{all}}} - \frac{\mathrm{AM}_{\mathrm{Spring-Summer}}}{\mathrm{AM}_{\mathrm{all}}}, \tag{2}$$

where the first and second terms represent the ratio of the frequency of AM precipitation events within the autumn-winter and spring-summer, respectively, to the total number of AM events within the whole period. S_D ranges from −1 to 1, with negative values indicating spring-summer-dominant events and positive values indicating autumn-winter-dominant events.

To compare the future changes in frequency between HCLIM3-E/G and HCLIM12-E/G from the CTRL to MC and LC periods, the number of hours (for hourly events) and days (for daily events) with precipitation exceeding the percentile-based thresholds (95th percentile) of the CTRL-period precipitation (>0.1 mm) is counted for all periods and each region. To maintain a consistent *y*-axis for the frequency of hourly and daily precipitation events within the same figure, the frequency of hourly precipitation events is converted to daily units.

3. Results

3.1. Future Changes in Intensity

Figure 2 illustrates the spatial distribution of the future change in annual Rx1h and Rx1d from CTRL to MC and LC based on HCLIM3-E, HCLIM3-G, HCLIM12-E, and HCLIM12-G. There is a notable increase in annual Rx1h and Rx1d in all regions from CTRL to MC and LC, particularly in the LC period with a statistically significant increase, as asserted by the *t*-test, in most of the grid points. This future increase of extremes is also clearly evidenced by the CF values, being greater than one in almost all regions (see Tables 1 and 2). Although the hourly and daily extremes increase in all regions and seasons, on average, as shown in the distribution for future change of Rx1h and Rx1d for HCLIM3-E/G and HCLIM12-E/G across eight regions (Figures S1 and S2 in Supporting Information S1), the daily extreme of HCLIM3-E and HCLIM12-E exhibit decrease in some seasons in the southern and south-western regions with CF less than 1 (Table 2). In contrast, the Rx1h and Rx1d consistently increase across eight regions from the HCLIM3-G and HCLIM12-G models, which also exhibits a stronger climate change signal with higher CF compared with the HCLIM3-E and HCLIM3-E models.

Among regions, the greatest change in annual and winter Rx1d is in northern-inland while the greatest summer change is in the northern-coastal region. These results are consistent with Hanssen-Bauer et al. (2017). Moreover, compared with Rx1d, a more pronounced increase of Rx1h, indicated by a larger CF, is seen in the HCLIM3-E/G and HCLIM12-E/G from CTRL to MC and LC in most regions except the southern and south-western regions, and for all seasons except winter. Previous studies, such as Ban et al. (2014) and Dyrrdal et al. (2023), have demonstrated that there is a greater change in sub-daily events than in daily events under global warming. This is

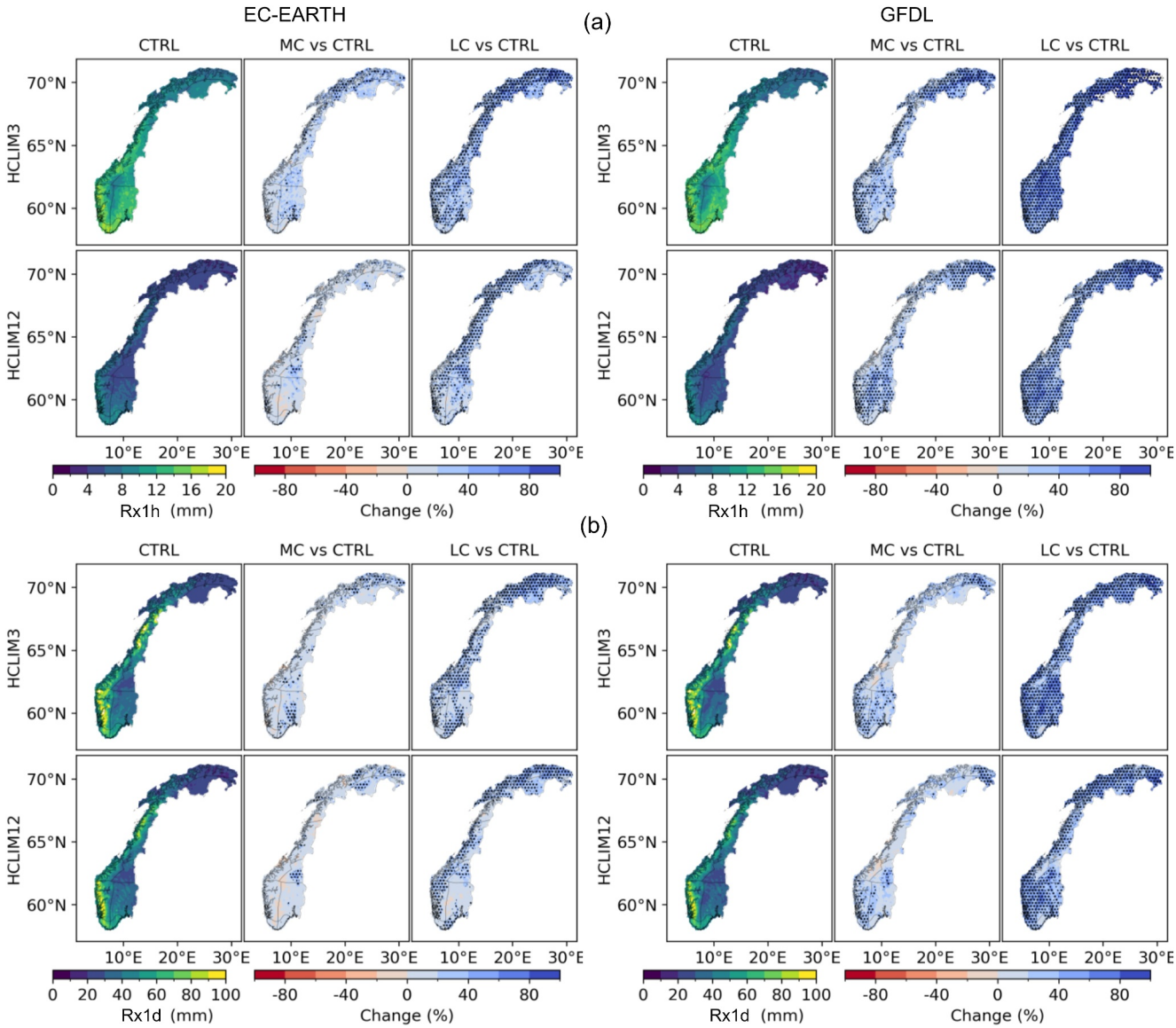

Figure 2. Extreme precipitation in the CTRL period and its future relative change for HCLIM3 and HCLIM12 forced by EC-EARTH and GFDL: (a) annual maximum 1-hr precipitation (Rx1h) and (b) annual maximum 1-day precipitation (Rx1d). The black dots indicate where the changes in extreme precipitation between CTRL and future time periods are statistically significant, using a *t*-test with 5% significance level.

consistent with the results presented here, although we note that in the HCLIM simulations it is subject to regional and seasonal dependence.

There is a discrepancy between HCLIM3 and HCLIM12 driven by EC-EARTH and GFDL models in terms of simulating future Rx1h and Rx1d. On average, HCLIM3-E and HCLIM3-G project a larger future change in Rx1h and Rx1d than HCLIM12-E and HCLIM12-G, especially on the hourly scale, as shown by the larger CF (Tables 1 and 2). The discrepancy between HCLIM3-E/G and HCLIM12-E/G is amplified from MC to LC. Particularly in winter, when large-scale weather systems dominate (Michel et al., 2021; Whan et al., 2020) and short-duration intense convective extremes occur less frequently, there is a reduced difference between HCLIM3-E/G and HCLIM12-E/G. On the daily scale, the change in annual Rx1d in HCLIM3-E/G is larger than that simulated by HCLIM12-E/G. The larger increase in Rx1d projected by HCLIM3-E/G is particularly pronounced in summer and autumn compared to HCLIM12-E/G, as shown in Figure S2 in Supporting Information S1 and Table 2.

Table 1
Climate Factor (CF) of Annual and Seasonal Rx1h From HCLIM3-E, HCLIM3-G, HCLIM12-E, and HCLIM12-G for Eight Regions

Hourly		Model	E	S	SW	W	MI	MCO	NI	NCO
Annual	MC	HCLIM3-E/G	[1.18,1.24]	[1.07,1.18]	[1.03,1.24]	[1.1,1.25]	[1.21,1.25]	[1.14,1.23]	[1.22,1.45]	[1.23,1.37]
		HCLIM12-E/G	[1.08,1.29]	[1.03,1.13]	[1.07,1.17]	[1.06,1.23]	[1.21,1.29]	[1.11,1.17]	[1.12,1.33]	[1.1,1.25]
	LC	HCLIM3-E/G	[[1.25,1.56]	[1.2,1.38]	[1.18,1.4]	[1.24,1.46]	[1.34,1.6]	[1.3,1.54]	[1.39,1.93]	[1.44,1.75]
		HCLIM12-E/G	[1.19,1.42]	[1.15,1.33]	[1.15,1.28]	[1.17,1.42]	[1.3,1.36]	[1.24,1.31]	[1.22,1.54]	[1.28,1.43]
Winter	MC	HCLIM3-E/G	[1.09,1.25]	[1.0,1.2]	[1.03,1.19]	[1.07,1.17]	[1.11,1.08]	[1.13,1.08]	[1.25,1.31]	[1.18,1.21]
		HCLIM12-E/G	[1.06,1.28]	[1,1.2]	[1.1,1.16]	[1.06,1.13]	[1.1,1.1]	[1.1,1.02]	[1.12,1.2]	[1.05,1.06]
	LC	HCLIM3-E/G	[1.28,1.46]	[1.17,1.34]	[1.19,1.34]	[1.11,1.33]	[1.14,1.23]	[1.21,1.17]	[1.48,1.56]	[1.41,1.36]
		HCLIM12-E/G	[1.23,1.45]	[1.2,1.35]	[1.21,1.32]	[1.17,1.3]	[1.17,1.24]	[1.23,1.1]	[1.31,1.45]	[1.32,1.18]
Spring	MC	HCLIM3-E/G	[1.23,1.25]	[1.14,1.15]	[1.18,1.25]	[1.2,1.19]	[1.19,1.29]	[1.2,1.11]	[1.43,1.18]	[1.34,1.1]
		HCLIM12-E/G	[1.15,1.13]	[**0.97**,1.16]	[1.07,1.05]	[1.14,1.1]	[1.15,1.1]	[1.18,1.02]	[1.23,1.16]	[1.27,1.08]
	LC	HCLIM3-E/G	[1.35,1.6]	[1.33,1.47]	[1.31,1.33]	[1.33,1.33]	[1.54,1.73]	[1.4,1.25]	[1.66,1.53]	[1.54,1.3]
		HCLIM12-E/G	[1.26,1.26]	[1.07,1.38]	[1.2,1.21]	[1.3,1.22]	[1.28,1.26]	[1.26,1.2]	[1.35,1.29]	[1.4,1.21]
Summer	MC	HCLIM3-E/G	[1.19,1.23]	[1.04,1.18]	[1.04,1.22]	[1.16,1.34]	[1.23,1.25]	[1.19,1.31]	[1.21,1.47]	[1.29,1.55]
		HCLIM12-E/G	[1.07,1.28]	[1.02,1.1]	[1.02,1.17]	[1.06,1.26]	[1.22,1.33]	[1.12,1.25]	[1.1,1.3]	[1.11,1.3]
	LC	HCLIM3-E/G	[1.25,1.54]	[1.14,1.33]	[1.18,1.38]	[1.29,1.6]	[1.34,1.6]	[1.35,1.71]	[1.38,1.99]	[1.52,2.09]
		HCLIM12-E/G	[1.15,1.32]	[1.06,1.25]	[1.08,1.23]	[1.14,1.44]	[1.33,1.36]	[1.28,1.41]	[1.19,1.55]	[1.3,1.52]
Autumn	MC	HCLIM3-E/G	[1.15,1.33]	[1.17,1.25]	[1.03,1.31]	[1.02,1.28]	[1.12,1.31]	[1.09,1.26]	[1.31,1.51]	[1.16,1.3]
		HCLIM12-E/G	[1.11,1.3]	[1.1,1.18]	[1.08,1.25]	[1.03,1.28]	[1.14,1.36]	[1.13,1.3]	[1.29,1.41]	[1.14,1.36]
	LC	HCLIM3-E/G	[1.37,1.58]	[1.31,1.32]	[1.18,1.49]	[1.23,1.54]	[1.37,1.78]	[1.32,1.52]	[1.5,1.66]	[1.4,1.49]
		HCLIM12-E/G	[1.27,1.52]	[1.26,1.29]	[1.2,1.38]	[1.19,1.48]	[1.3,1.59]	[1.3,1.48]	[1.41,1.58]	[1.36,1.54]

Note. Bold represents the extreme precipitation decrease in the future MC and LC period compared with CTRL period, with CF less than 1. The values to the left of the comma inside the square brackets are the results from HCLIM3-E or HCLIM12-E while the values to the right of the comma are the results from HCLIM3-G or HCLIM12-G.

3.2. Future Changes in Frequency

Figure 3 illustrates the mean frequency of hourly and daily extreme precipitation exceeding the 95th percentile threshold derived from the CTRL-period. Overall, all models (HCLIM3-E/G and HCLIM12-E/G) simulate an increase in both hourly and daily extreme precipitation frequencies from the CTRL to the MC and LC periods across all eight regions.

During all three periods (CTRL, MC, and LC) HCLIM12-E/G generally simulates higher frequencies of extreme precipitation than HCLIM3-E/G in most regions. An exception is found in the northern-inland region, where HCLIM3-E/G shows similar frequencies of hourly extremes compared to HCLIM12-E/G. While daily extreme events are more frequent than hourly ones in all models and regions, the inter-model differences in simulating frequency are of similar magnitude for both timescales (see Figure 3).

The projected changes from CTRL to future periods (MC and LC) are also comparable between HCLIM3-E/G and HCLIM12-E/G for both hourly and daily extremes, as shown by similar slopes in frequency increase across all regions. Notably, all models project a slightly steeper increase in the frequency of daily extreme than hourly ones.

3.3. Future Changes in Seasonality

The seasonality index (S_D) of Rx1h and Rx1d from HCLIM3 and HCLIM12 driven by EC-EARTH and GFDL models in the future is shown in Figure 4. In most regions, both HCLIM3-E/G and HCLIM12-E/G suggest that hourly precipitation extremes occur predominantly in spring and summer, the exception being HCLIM12-E/G in the southern, south-western, and western regions, where S_D is positive or near zero (mostly autumn-winter dominant) in HCLIM12-E/G. For daily extremes, spring-summer events dominate in the eastern, middle-inland, and northern-inland regions while autumn-winter events dominate elsewhere.

Table 2
Climate Factor (CF) of Annual and Seasonal Rx1d From HCLIM3-E, HCLIM3-G, HCLIM12-E, and HCLIM12-G for Eight Regions

Daily		Model	E	S	SW	W	MI	MCO	NI	NCO
Annual	MC	HCLIM3-E/G	[1.14,1.23]	[1.16,1.17]	[1.04,1.24]	[1.06,1.21]	[1.13,1.16]	[1.1,1.1]	[1.12,1.19]	[1.16,1.21]
		HCLIM12-E/G	[1.06,1.19]	[1.09,1.12]	[1.03,1.23]	[1.03,1.21]	[1.15,1.22]	[1.06,1.07]	[1.19,1.18]	[1.14,1.19]
	LC	HCLIM3-E/G	[1.18,1.5]	[1.3,1.2]	[1.14,1.47]	[1.17,1.44]	[1.27,1.51]	[1.24,1.37]	[1.32,1.49]	[1.31,1.45]
		HCLIM12-E/G	[1.09,1.37]	[1.23,1.18]	[1.14,1.41]	[1.16,1.43]	[1.19,1.36]	[1.2,1.29]	[1.27,1.47]	[1.27,1.41]
Winter	MC	HCLIM3-E/G	[1.17,1.28]	[1.17,1.19]	[1.09,1.22]	[1.1,1.19]	[1.16,1.07]	[1.12,1.04]	[1.32,1.29]	[1.18,1.13]
		HCLIM12-E/G	[1.16,1.24]	[1.12,1.09]	[1.15,1.21]	[1.14,1.18]	[1.16,1.05]	[1.15,1.01]	[1.37,1.22]	[1.2,1.08]
	LC	HCLIM3-E/G	[1.34,1.38]	[1.29,1.24]	[1.23,1.41]	[1.16,1.38]	[1.19,1.19]	[1.29,1.2]	[1.3,1.46]	[1.39,1.33]
		HCLIM12-E/G	[1.31,1.31]	[1.35,1.23]	[1.21,1.43]	[1.17,1.32]	[1.19,1.13]	[1.23,1.12]	[1.37,1.47]	[1.36,1.29]
Spring	MC	HCLIM3-E/G	[1.13,1.17]	[**0.98**,1.3]	[1.1,1.21]	[1.1,1.13]	[1.07,1.09]	[1.11,1.05]	[1.08,1.08]	[1.24,1.13]
		HCLIM12-E/G	[1.06,1.13]	[**0.96**,1.31]	[1.13,1.17]	[1.04,1.08]	[1.1,1.03]	[1.12,1.02]	[1.07,1.15]	[1.28,1.13]
	LC	HCLIM3-E/G	[1.14,1.4]	[1.06,1.5]	[1.08,1.34]	[1.2,1.26]	[1.17,1.31]	[1.17,1.29]	[1.25,1.24]	[1.3,1.28]
		HCLIM12-E/G	[1.14,1.34]	[1.11,1.55]	[1.21,1.31]	[1.18,1.24]	[1.23,1.19]	[1.18,1.27]	[1.32,1.29]	[1.35,1.29]
Summer	MC	HCLIM3-E/G	[1.12,1.2]	[1.04,1.13]	[1,1.14]	[1.14,1.2]	[1.19,1.23]	[1.15,1.25]	[1.11,1.21]	[1.13,1.27]
		HCLIM12-E/G	[1.03,1.2]	[**0.92**,1.16]	[1,1.07]	[1.11,1.2]	[1.19,1.28]	[1.15,1.25]	[1.17,1.16]	[1.11,1.2]
	LC	HCLIM3-E/G	[1.15,1.44]	[1.11,1.1]	[1.04,1.17]	[1.18,1.41]	[1.32,1.6]	[1.28,1.5]	[1.32,1.54]	[1.33,1.54]
		HCLIM12-E/G	[1.03,1.23]	[**0.97**,1.04]	[**0.98**,1.11]	[1.17,1.4]	[1.22,1.4]	[1.33,1.39]	[1.28,1.47]	[1.33,1.43]
Autumn	MC	HCLIM3-E/G	[1.15,1.18]	[1.25,1.15]	[1.08,1.31]	[1.01,1.28]	[1.07,1.14]	[1.11,1.21]	[1.12,1.24]	[1.13,1.23]
		HCLIM12-E/G	[1.09,1.14]	[1.19,1.13]	[1.08,1.27]	[**0.98**,1.24]	[1.02,1.21]	[1.13,1.23]	[1.06,1.23]	[1.13,1.27]
	LC	HCLIM3-E/G	[1.28,1.43]	[1.33,1.23]	[1.21,1.56]	[1.22,1.54]	[1.26,1.42]	[1.27,1.52]	[1.25,1.45]	[1.26,1.44]
		HCLIM12-E/G	[1.2,1.4]	[1.22,1.23]	[1.21,1.46]	[1.21,1.5]	[1.14,1.37]	[1.33,1.45]	[1.2,1.46]	[1.25,1.51]

Note. Bold represents the extreme precipitation decrease in the future MC and LC period compared with CTRL period, with CF less than 1. The values to the left of the comma inside the square brackets are the results from HCLIM3-E or HCLIM12-E while the values to the right of the comma are the results from HCLIM3-G or HCLIM12-G.

The seasonality of extreme precipitation has no overall shift (change in the sign of the seasonality index) from CTRL to future periods in most regions, with the exceptions of HCLIM3-E/G in the western and HCLIM12-E/G in the southern regions. Specifically, HCLIM3-E and HCLIM3-G in the western region project a shift in the seasonality of hourly extremes from autumn-winter to spring-summer, with this shift being statistically significant. Similarly, HCLIM12-E and HCLIM12-G in the southern region project a shift from spring-summer to autumn-winter. From CTRL to MC or LC periods, the change in seasonality is significant by *t*-test in most regions, with a few exceptions. Specifically, a significant change in the seasonality of hourly extremes is seen in the eastern, southern, western, middle-coastal, and northern-inland regions. In contrast, the seasonality of hourly extremes in the middle-inland region, as simulated by the HCLIM3-E/G and HCLIM12-E/G, does not show a significant change in the future. Furthermore, no significant changes in the seasonality of hourly extremes are shown for HCLIM3-E and HCLIM3-G in the south-western region, or for HCLIM12-E and HCLIM12-G in the northern-coastal region.

Although the value of the S_D of extremes differs between HCLIM3-E/G and HCLIM12-E/G, the sign of the S_D remains consistent between the models in most regions, with a few exceptions for hourly extremes. Specifically, in the southern, south-western, and western regions, HCLIM12-E/G indicate that the hourly extremes are primary dominated by autumn-winter, whereas HCLIM3-E/G shows these extremes to be dominated by spring-summer. Compared with daily extremes, the disparity in the value of the S_D between HCLIM3-E/G and HCLIM12-E/G is more pronounced on an hourly basis. HCLIM3-E/G also simulates a higher proportion of hourly events occurring in spring-summer for CTRL, MC, and LC periods, indicated by smaller S_D compared with HCLIM12-E/G. In some regions (including western, middle-coastal, northern-inland, and northern-coastal regions), hourly S_D under CTRL period is very similar for HCLIM3-E/G and HCLIM12-E/G while the differences between them become more apparent with climate change. Additionally, the smaller S_D of Rx1h relative to that of Rx1d implies a higher

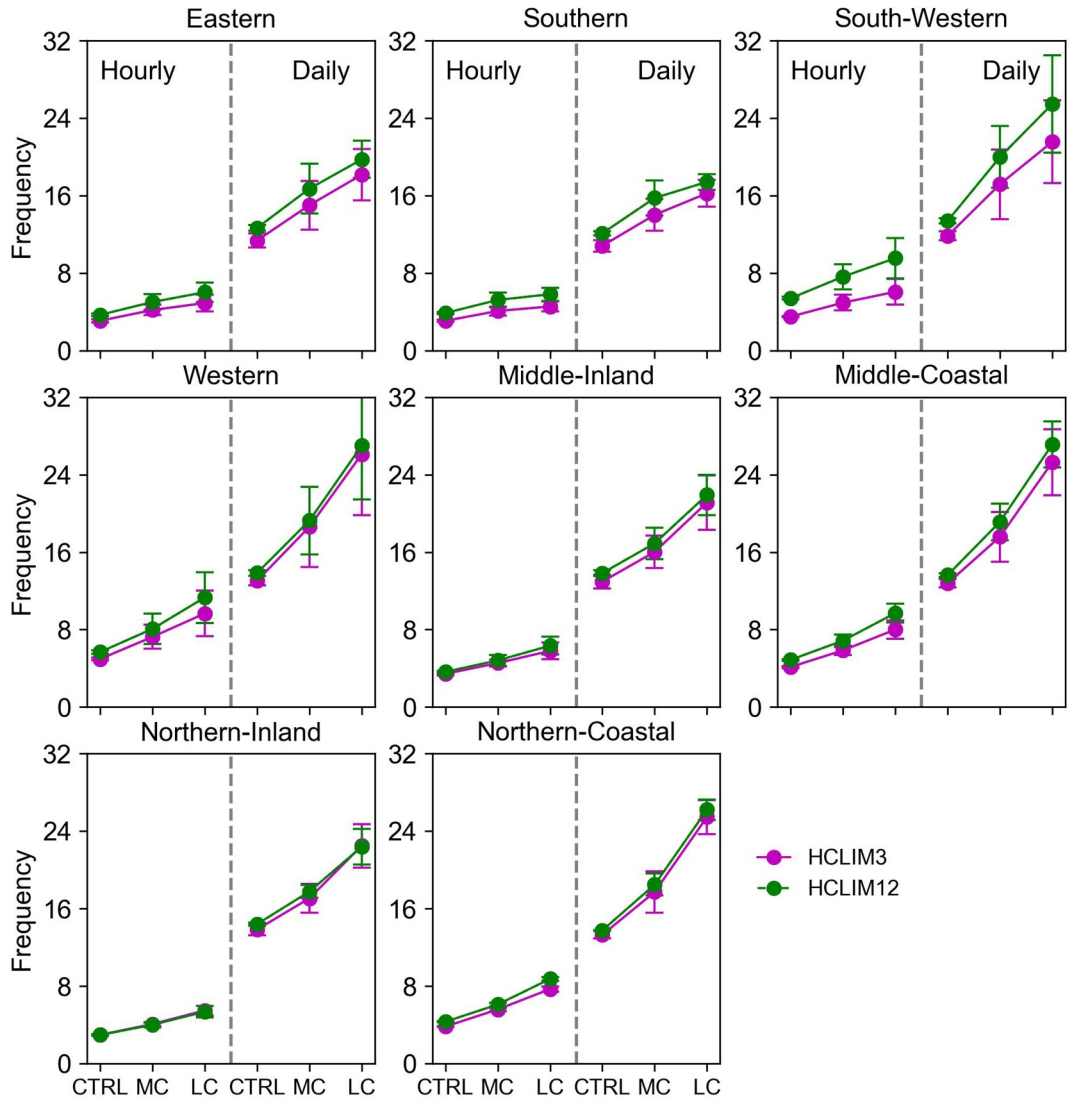

Figure 3. Mean frequency of the extreme precipitation across eight regions for the CTRL, MC, and LC periods. Error bars indicate frequency from HCLIM models driven by EC-EARTH and GFDL, the filled circle where the lines intersect the error bars represent the average frequency of the two models.

proportion of hourly extreme precipitation events occurring in spring-summer for CTRL, MC, and LC periods across eight regions.

3.4. Case Study of Bergen Localized Municipality for Extreme Precipitation

3.4.1. Hourly Extreme Precipitation Evaluation in Bergen Municipality

Although many studies suggested that CPRCMs can improve the simulation of extreme weather events at the local scale, there has been little focus on analyzing their results at the municipal scale. For example, local practitioners such as urban planners in municipalities need local climate information to identify potential future climate risks in specific communities. By entering into these scales with climate projections, practitioners can formulate targeted policies and regulations based on specific risks and vulnerabilities. Based on the results presented in Section 3.3, we see that both HCLIM3-E/G and HCLIM12-E/G show consistent positive seasonality in Rx1h for the western region during the CTRL period. Under future climate scenarios, the seasonality in HCLIM3-E/G turns from positive to negative while HCLIM12-E/G maintains its original sign.

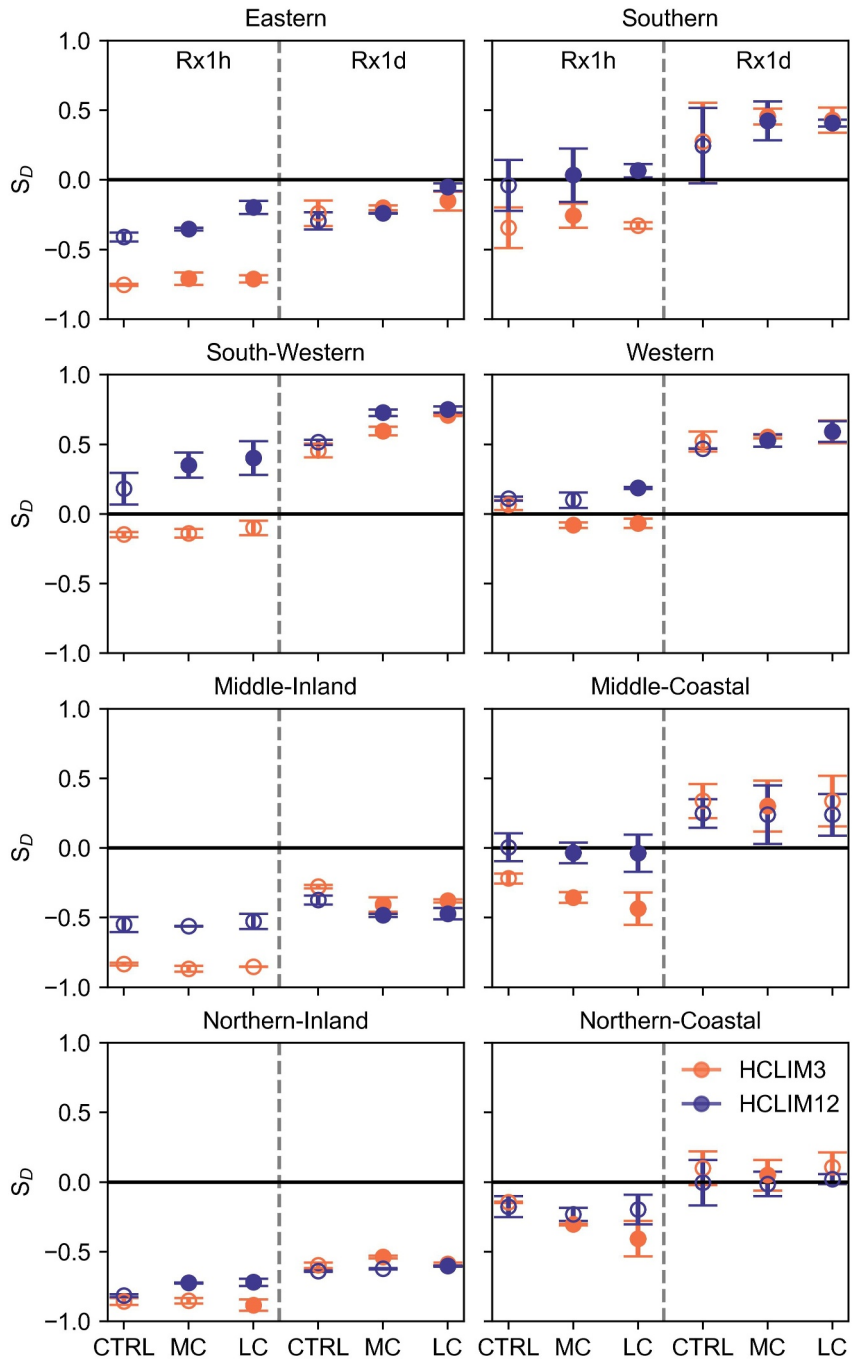

Figure 4. S_D of annual Rx1h and annual Rx1d simulated by HCLIM3 and HCLIM12 forced by EC-EARTH and GFDL in the CTRL, MC, and LC periods. Error bars indicate S_D from HCLIM models driven by EC-EARTH and GFDL. The circle represents the average S_D between EC-EARTH and GFDL driven model. A filled circle indicates that the change of the average S_D is statistically significant (t-test) between MC or LC and CTRL period.

To explore this further, we choose to demonstrate the model behavior over the area of Bergen municipality, located in the western region for a case study to analyze future changes in Rx1h at the municipal level, with the spatial distribution of Bergen's districts presented in Figure S3 in Supporting Information S1. Bergen, with a maritime climate, characterized by mild winters and cool summers, stands out as the city with the highest precipitation amount in Europe. Its coastal location and the surrounding mountains often create orographic uplift that intensifies precipitation (Dyrrdal et al., 2016). Figure 5 shows the topography in the areas of Bergen municipality

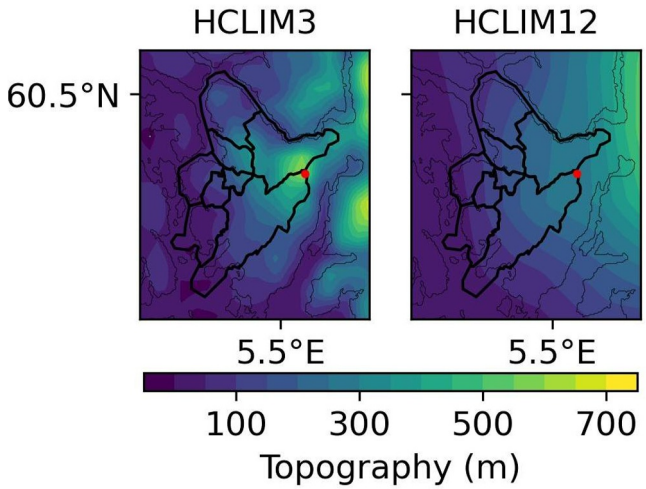

Figure 5. Spatial distribution of the topography in Bergen from HCLIM3 and HCLIM12. The red dot indicates the location of Gullfjellet. The observed elevation of Gullfjellet is 914 m.

in HCLIM3 and HCLIM12. It can be clearly seen that HCLIM3 better resolves the surrounding topography while in HCLIM12 it is very smooth. Precipitation from the SeNorge2 (SeNorge) gridded data set, covering Norway with 1-hr and 1 km resolution precipitation since 2010 (Lussana et al., 2018), is used as the observation data set to evaluate the performance of climate models. A comparison of Rx1h simulated by HCLIM with SeNorge observations shows that it is represented more realistically in HCLIM3 while HCLIM12 shows a large underestimation (Figure 6). Notably, HCLIM3 seems to overestimate precipitation in areas with elevated orography, in the eastern part of the small domain (Figure 6) and underestimates in the low-altitude southwestern part. This gave us confidence to look more closely at the HCLIM3 projections at the municipal level.

3.4.2. Future Change of Hourly Extreme Precipitation in Bergen Municipality

Across eight districts, annual Rx1h increases from CTRL to LC, especially for HCLIM3-G, as shown in Figure 7. In this test case, we calculated the climate factor (CF) for annual and seasonal Rx1h from HCLIM3-E/G and HCLIM12-E/G for eight districts in the municipality, as shown in the Tables S1 and S2 in Supporting Information S2. On average, the annual and seasonal Rx1h are projected to increase in all eight districts with HCLIM3-E/G and HCLIM12-E/G, indicated by CF greater than 1. A comparison of the CF between HCLIM3-E/G and HCLIM12-E/G indicates that the differences in change signals between districts are less pronounced. Specifically, the maximum discrepancy in CF between districts is less than 0.1, whereas the difference in CF between HCLIM3 and HCLIM12 is approximately 0.5, indicating that the model uncertainty is much bigger than the local variability in climate change response. Regarding the change in seasonal Rx1h, the results indicate that, on average, HCLIM3-E/G and HCLIM12-E/G-E/G project the largest change in summer, followed by autumn in the MC period, as shown in Figure S4 in Supporting Information S1. Specifically, the smallest increase in extremes is observed in winter across the eight districts while the largest increase occurs in autumn or summer. By the end of the century, the CF varies between approximately 1.10 and 1.40 on average depending on the season and district.

4. Discussion

Assessing future changes of extreme precipitation is crucial for effective infrastructure protection and planning appropriate flood defenses. Hanssen-Bauer et al. (2017) showed that heavy precipitation at a daily scale will be more intense in all regions of Norway and for all seasons by the end of the century based on RCMs with a horizontal grid spacing of ∼12 km (Jacob et al., 2020). In this study, we found a future increase of the intensity of hourly and daily extremes at annual and seasonal scale in most regions from CPRCMs and RCMs, with a few exceptions for daily extremes. Specifically, HCLIM driven by EC-EARTH shows a slight decrease in spring and

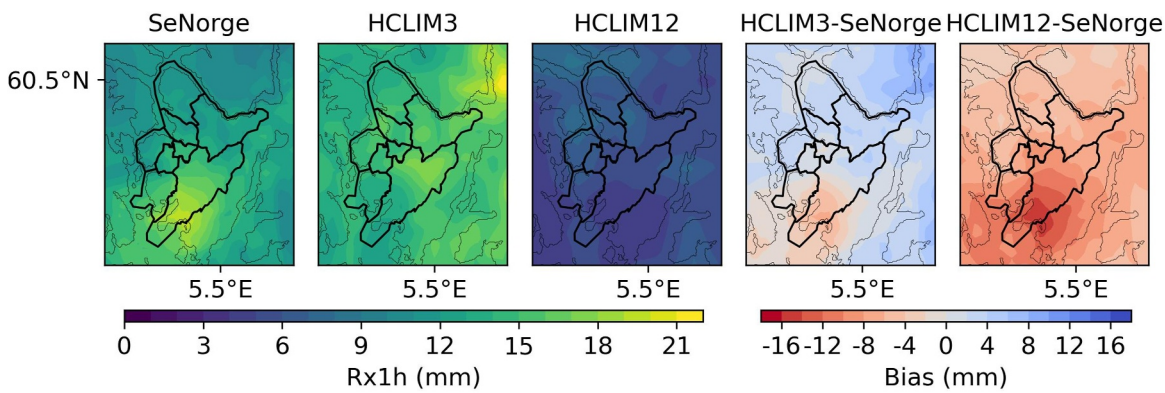

Figure 6. Spatial distribution of hourly extreme precipitation from SeNorge, HCLIM3, and HCLIM12 for Bergen municipality.

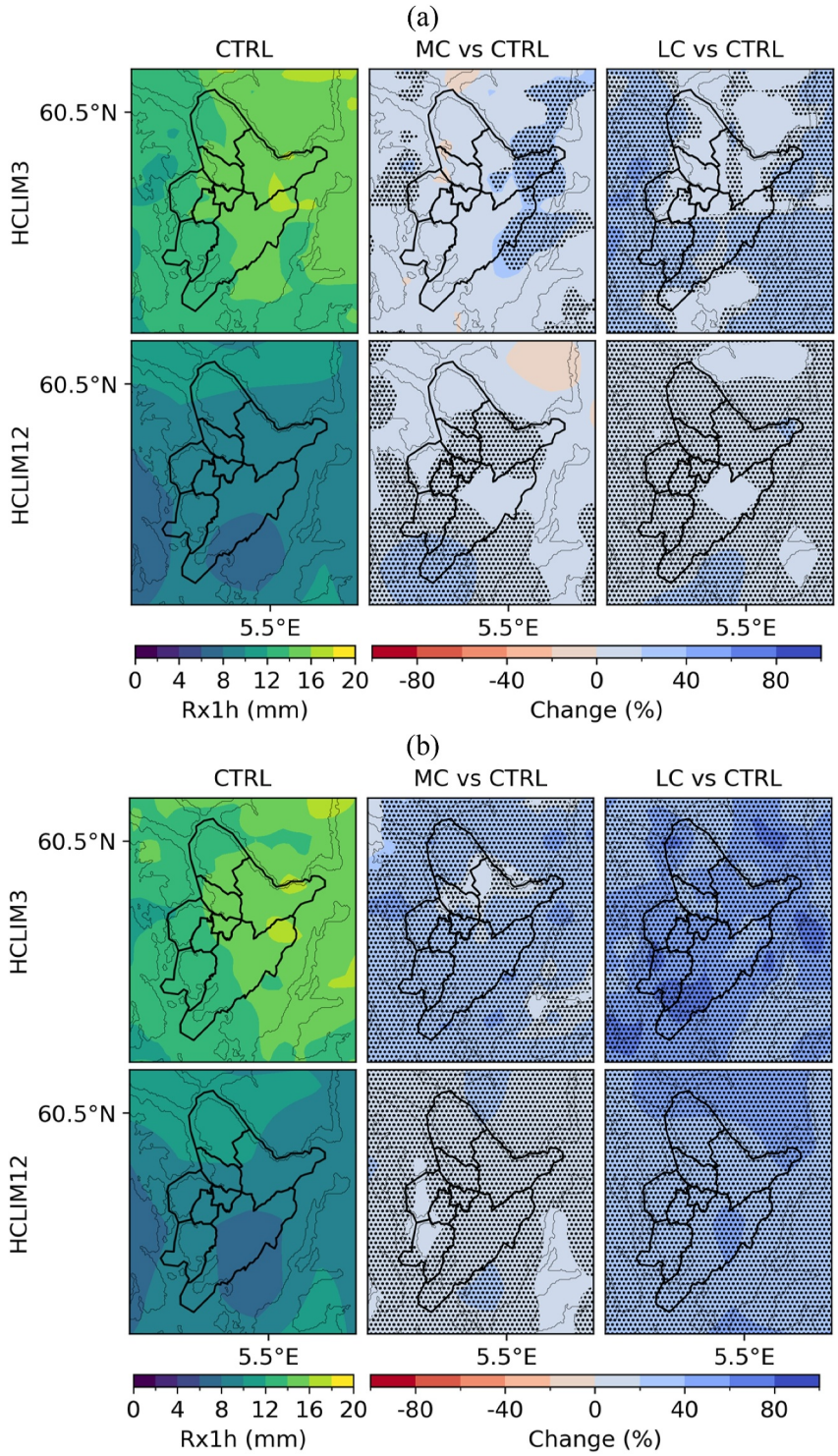

Figure 7. Hourly extremes (Rx1h) in the CTRL period and its future relative change for HCLIM3 and HCLIM12 driven by (a) EC-EARTH and (b) GFDL model. The black dots indicate where the changes in extreme precipitation between CTRL and future time periods are statistically significant, using a *t*-test with 5% significance level.

summer Rx1d, primarily in the southern and south-western regions. In contrast, HCLIM models driven by GFDL consistently project increases across all eight regions in the future. These results may be attributed to the fact that EC-EARTH warms less and experiences a smaller increase in precipitation compared to GFDL. Lind et al. (2022)

and Dyrrdal et al. (2023) indicated that moisture availability is playing a role in limiting the increase of extremes in the southern parts of the Fenno-Scandinavia region. As indicated by Wang et al. (2019), specific humidity and winds can be used to estimate the moisture transport. Here, we initially compared the change of specific humidity at a specific level (e.g., 500 hPa) between EC-EARTH and GFDL, as shown in Figure S5 in Supporting Information S1, which shows that EC-EARTH projects a smaller increase of specific humidity than GFDL model in the future. However, additional factors must be considered to fully understand the mechanisms driving changes in extreme events in the future research.

By investigating the difference between CPRCMs and RCMs in simulating extreme precipitation at finer regional scale, we found that the discrepancy can vary substantially depending on geographic location and season. Specifically, the differences between HCLIM3-E/G and HCLIM12-E/G in projections of winter Rx1d and Rx1h are smaller than in other seasons, noting that winter precipitation is mainly dominated by large-scale weather systems. Prein et al. (2013) also noted that the differences between RCMs and CPRCMs in capturing winter precipitation are negligible. In contrast, in the southern region, the increase in summer Rx1d by HCLIM3-E/G agrees well with the findings of Poujol et al. (2021) and Dyrrdal et al. (2023) while HCLIM12-E projects a decreasing with CF less than 1. This further confirms the benefit of CPRCMs in projecting future change in extreme precipitation at the regional scale, especially in summer dominated by strong deep convective activity.

From historical period to future period, although the seasonality index of extremes exhibits significant change in some regions, the seasonality of extreme precipitation does not undergo a shift in the sign of the seasonality index in these simulations, except for hourly extremes in the southern and western regions. In western region, extreme precipitation is largely driven by atmospheric rivers (Azad & Sorteberg, 2017), particularly during winter (Whan et al., 2020), while summer convective activity is also strong (Poujol et al., 2021). The role of atmospheric rivers and convective activity in different seasons, and their influence on the seasonality shift in the western region, should be explored in future research.

Furthermore, CPRCMs show a stronger response to climate change than RCMs in simulating extreme precipitation in Norway, which is consistent with the findings of Dyrrdal et al. (2023) and Lind et al. (2022) at the country scale. Furthermore, Chan et al. (2020) and Fosser et al. (2024) demonstrated that CPRCMs project stronger increase of precipitation extremes than coarser RCMs in the future in Europe. Additionally, we also found that the discrepancy between CPRCMs and RCMs in projecting the future change of extreme precipitation varies with the timescale. Compared with the change of hourly extremes, there is no substantial distinction between HCLIM3-E/G and HCLIM12-E/G on a daily scale, indicating that CPRCMs can provide a valuable means of capturing the change of convection events, as short duration events are most closely linked to convection (Kendon et al., 2017). This result is consistent with the findings of Adinolfi et al. (2021), who conducted a Europe-wide study and determined that the primary distinction between CPRCMs and RCMs is the enhanced characterization of hourly extremes.

The higher frequency of the extreme precipitation events simulated by HCLIM12-E/G compared with HCLIM3-E/G during CTRL, MC, and LC periods may stem from RCMs overestimating the frequency. As demonstrated by Lind et al. (2020), Lucas-Picher et al. (2024), and Ha et al. (2024) in European studies, CPRCMs generally simulate fewer wet days than RCMs. Kendon et al. (2023) further showed that RCMs significantly overestimate the frequency of hourly extreme precipitation events above high thresholds in the UK across historical and future periods when compared with CPRCMs. Our findings complement this body of research by illustrating that the differences between RCMs and CPRCMs in extreme precipitation frequency projections align with their disparities in wet-day counts. Additionally, the comparable increase in the frequency of hourly and daily extreme precipitation is projected between HCLIM3-E/G and HCLIM12-E/G from CTRL to MC and LC periods, enhances understanding of future extreme precipitation frequency changes between RCM and CPRCM frameworks.

GCMs have significant uncertainties, so multi-model ensembles are needed to improve the accuracy and robustness (Ganguly & Arya, 2023). However, due to the high computational demands of CPRCMs, existing studies rarely consider multi-model ensembles. Assessing precipitation changes at the very local scale remains a challenge also in this study due to the limited number of simulations (two GCMs), making it difficult to establish certainty in projected changes, particularly for extreme events. To address this uncertainty, incorporating multi-model ensembles of CPRCMs would be necessary to better assess uncertainties in projections of future changes of extreme precipitation. Future research could benefit from longer simulation periods or the development of new indices, such as percentile-based indices, to better capture the variability and seasonality of extreme events. For

the local scale, future research could consider adopting a targeted approach by selecting specific extreme events or weather scenarios based on a storyline framework. This would enable a clearer demonstration of the differences in how CPRCMs and RCMs simulate local-scale precipitation patterns and their responses to climate change, thereby providing deeper insights into the potential impacts on municipalities and regions. Additionally, it is important to acknowledge the uncertainty inherent in conducting statistical tests or analyzing extremes for seasonality of maxima from the limited CPRCMs simulations (20 years).

5. Conclusions

In this study, we conduct a comprehensive analysis of daily and hourly extreme precipitation projections across eight distinct regions in Norway, utilizing the convection-permitting regional climate model HCLIM3. We compare these results with a coarse scale model (HCLIM12) that utilizes a convection parameterization scheme. Both models are driven by EC-EARTH and GFDL under the RCP8.5 scenario, covering the periods 1986–2005 (CTRL), 2041–2060 (MC), and 2081–2100 (LC).

The key conclusions are:

1. The intensity of hourly and daily extremes is projected to increase in most regions of Norway, except for the daily extremes from HCLIM3-E and HCLIM12-E in the southern areas of Norway (including southern and south-western regions). HCLIM models driven by GFDL model also show larger increase in extremes than that driven by EC-EARTH, which is likely associated with smaller increases in atmospheric temperature and humidity in EC-EARTH compared with GFDL. In comparison to daily extremes, the intensity of Rx1h demonstrates a more pronounced increase in most regions and seasons except for winter, suggesting a larger response of hourly extremes to warming. Additionally, the frequency of both hourly and daily extreme precipitation events increases from CTRL to MC and LC period across all eight regions. However, the seasonality exhibits no shifting on either the daily or hourly timescales in most regions, except for the hourly extremes in the southern and western regions.
2. The discrepancies between HCLIM3-E/G and HCLIM12-E/G in projecting future changes in extreme precipitation are more substantial for the hourly than the daily time scale. Generally, HCLIM3-E/G projects larger increase of hourly extreme precipitation than HCLIM12-E/G over most regions and seasons except winter in Norway, and a higher incidence of spring-summer dominated hourly precipitation events. Across all eight regions, the changes in the frequency of hourly and daily extreme events from CTRL to future periods (MC and LC) are comparable between HCLIM3-E/G and HCLIM12-E/G for both hourly and daily extremes.
3. At the municipal scale of the west coast city of Norway (Bergen), the high-resolution convection-permitting model driven by GCMs shows larger change of extreme precipitation than traditional climate model in the future, except in some local districts in winter. Importantly, a larger model uncertainty than local differences is also seen in the results.

In conclusion, our comprehensive analysis offers a nuanced understanding of the potential future changes in extreme precipitation at regional and local scales in Norway. The higher sensitivity of CPRCMs compared with RCMs, along with regional and local variations, suggests that we may be underestimating future hourly precipitation extremes by RCMs. We conclude by emphasizing the need for localized assessments to inform adaptive strategies in the face of changing precipitation patterns.

Conflict of Interest

The authors declare no conflicts of interest relevant to this study.

Data Availability Statement

The extreme precipitation indices of HCLIM3-E/G and HCLIM12-E/G are available at (Xie, 2025a) [Dataset]. GCMs (EC-EARTH and GFDL-CM3) are accessible at https://aims2.llnl.gov/search [Dataset]. The codes for this study are available at (Xie, 2025b) [Software]. Some parts of the ALADIN–HIRLAM codes can be obtained by non-members through specific licenses, such as in OpenIFS (Integrated Forecasting System, https://confluence.ecmwf.int/display/OIFS, Carver, 2022) [Software] and Open-SURFEX (Surface Externalisée; https://www.umr-cnrm.fr/surfex, SURFEX, 2022) [Software]. Figures and codes were made with the Python version 3.9.7,

available at https://www.python.org [Software]. All simulation data in this paper are available from the authors upon request (luli@norceresearch.no).

Acknowledgments

We would like to thank Ozan Mert Göktürk, for his great supports as data manager of the EU Impetus4change (I4C) project. Also, thanks to Andreas Dobler for providing the HCLIM3 and HCLIM12 data and his earlier suggestions on the work. This research was supported by the European Union's Horizon 2020 research, innovation programme under grant agreement no. 101081555 (IMPETUS4CHANGE). The computer resources where available through the RCN's program for supercomputing (NOTUR/NORSTORE); projects NN10014K and NS10014K. This work uses data from the NorCP project, which is a Nordic collaboration involving climate modeling groups from the Danish Meteorological Institute (DMI), Finnish Meteorological Institute (FMI), Norwegian Meteorological Institute (MET Norway), and the Swedish Meteorological and Hydrological Institute (SMHI).

References

Adinolfi, M., Raffa, M., Reder, A., & Mercogliano, P. (2021). Evaluation and expected changes of summer precipitation at convection permitting scale with COSMO-CLM over Alpine space. *Atmosphere*, *12*(1), 54. https://doi.org/10.3390/atmos12010054

Azad, R., & Sorteberg, A. (2017). Extreme daily precipitation in coastal Western Norway and the link to atmospheric rivers. *Journal of Geophysical Research: Atmospheres*, *122*(4), 2080–2095. https://doi.org/10.1002/2016jd025615

Ban, N., Schmidli, J., & Schär, C. (2014). Evaluation of the convection-resolving regional climate modeling approach in decade-long simulations. *Journal of Geophysical Research: Atmospheres*, *119*(13), 7889–7907. https://doi.org/10.1002/2014JD021478

Carver, G. (2022). OpenIFS home [Software]. *ECMWF*. Retrieved from https://confluence.ecmwf.int/display/OIFS

Chan, S. C., Kahana, R., Kendon, E. J., & Fowler, H. J. (2018). Projected changes in extreme precipitation over Scotland and Northern England using a high-resolution regional climate model. *Climate Dynamics*, *51*(9), 3559–3577. https://doi.org/10.1007/s00382-018-4096-4

Chan, S. C., Kendon, E. J., Berthou, S., Fosser, G., Lewis, E., & Fowler, H. J. (2020). Europe-wide precipitation projections at convection permitting scale with the unified model. *Climate Dynamics*, *55*(3), 409–428. https://doi.org/10.1007/s00382-020-05192-8

Chan, S. C., Kendon, E. J., Fowler, H. J., Blenkinsop, S., & Roberts, N. M. (2014). Projected increases in summer and winter UK sub-daily precipitation extremes from high-resolution regional climate models. *Environmental Research Letters*, *9*(8), 084019. https://doi.org/10.1088/1748-9326/9/8/084019

Chapman, S., Bacon, J., Birch, C. E., Pope, E., Marsham, J. H., Msemo, H., et al. (2023). Climate change impacts on extreme rainfall in eastern Africa in a convection-permitting climate model. *Journal of Climate*, *36*(1), 93–109. https://doi.org/10.1175/JCLI-D-21-0851.1

Chen, D., Dai, A., & Hall, A. (2021). The convective-to-total precipitation ratio and the "drizzling" bias in climate models. *Journal of Geophysical Research: Atmospheres*, *126*(16), e2020JD034198. https://doi.org/10.1029/2020JD034198

Dyrrdal, A. V., Médus, E., Dobler, A., Hodnebrog, Ø., Arnbjerg-Nielsen, K., Olsson, J., et al. (2023). Changes in design precipitation over the Nordic-Baltic region as given by convection-permitting climate simulations. *Weather and Climate Extremes*, *42*, 100604. https://doi.org/10.1016/j.wace.2023.100604

Dyrrdal, A. V., Thomas, S., Frode, S., & Førland, E. J. (2016). Estimating extreme areal precipitation in Norway from a gridded dataset. *Hydrological Sciences Journal*, *61*(3), 483–494. https://doi.org/10.1080/02626667.2014.947289

Efron, B. (1969). Student's t-test under symmetry conditions. *Journal of the American Statistical Association*, *64*(328), 1278–1302. https://doi.org/10.2307/2286068

Fosser, G., Gaetani, M., Kendon, E. J., Adinolfi, M., Ban, N., Belušić, D., et al. (2024). Convection-permitting climate models offer more certain extreme rainfall projections. *npj Climate and Atmospheric Science*, *7*(1), 51. https://doi.org/10.1038/s41612-024-00600-w

Fosser, G., Kendon, E. J., Stephenson, D., & Tucker, S. (2020). Convection-permitting models offer promise of more certain extreme rainfall projections. *Geophysical Research Letters*, *47*(13). https://doi.org/10.1029/2020gl088151

Ganguly, T., & Arya, D. S. (2023). A novel framework for a multimodel ensemble of GCMs and its application in the analysis of projected extremes. *International Journal of Climatology*, *43*(15), 7308–7325. https://doi.org/10.1002/joc.8266

Ha, M. T., Bastin, S., Drobinski, P., Fita, L., Polcher, J., Bock, O., et al. (2024). Precipitation frequency in Med-CORDEX and EURO-CORDEX ensembles from 0.44° to convection-permitting resolution: Impact of model resolution and convection representation. *Climate Dynamics*, *62*(6), 4515–4540. https://doi.org/10.1007/s00382-022-06594-6

Hanel, M., & Buishand, T. A. (2010). On the value of hourly precipitation extremes in regional climate model simulations. *Journal of Hydrology*, *393*(3), 265–273. https://doi.org/10.1016/j.jhydrol.2010.08.024

Hanssen-Bauer, I., Førland, E., Haddeland, I., Hisdal, H., Lawrence, D., Mayer, S., et al. (2017). Climate in Norway 2100.

Hodnebrog, Ø., Marelle, L., Alterskjær, K., Wood, R. R., Ludwig, R., Fischer, E. M., et al. (2019). Intensification of summer precipitation with shorter time-scales in Europe. *Environmental Research Letters*, *14*(12), 124050. https://doi.org/10.1088/1748-9326/ab549c

Huo, R., Li, L., Engeland, K., Xu, C.-Y., Chen, H., Paasche, Ø., & Guo, S. (2022). Changing flood dynamics in Norway since the last millennium and to the end of the 21st century. *Journal of Hydrology*, *613*, 128331. https://doi.org/10.1016/j.jhydrol.2022.128331

Jacob, D., Teichmann, C., Sobolowski, S., Katragkou, E., Anders, I., Belda, M., et al. (2020). Regional climate downscaling over Europe: Perspectives from the EURO-CORDEX community. *Regional Environmental Change*, *20*(2), 51. https://doi.org/10.1007/s10113-020-01606-9

Kendon, E. J., Ban, N., Roberts, N. M., Fowler, H. J., Roberts, M. J., Chan, S. C., et al. (2017). Do convection-permitting regional climate models improve projections of future precipitation change? *Bulletin of the American Meteorological Society*, *98*(1), 79–93. https://doi.org/10.1175/BAMS-D-15-0004.1

Kendon, E. J., Fischer, E. M., & Short, C. J. (2023). Variability conceals emerging trend in 100yr projections of UK local hourly rainfall extremes. *Nature Communications*, *14*(1), 1133. https://doi.org/10.1038/s41467-023-36499-9

Kendon, E. J., Stratton, R. A., Tucker, S., Marsham, J. H., Berthou, S., Rowell, D. P., & Senior, C. A. (2019). Enhanced future changes in wet and dry extremes over Africa at convection-permitting scale. *Nature Communications*, *10*(1), 1794. https://doi.org/10.1038/s41467-019-09776-9

Knist, S., Goergen, K., & Simmer, C. (2020). Evaluation and projected changes of precipitation statistics in convection-permitting WRF climate simulations over Central Europe. *Climate Dynamics*, *55*(1–2), 325–341. https://doi.org/10.1007/s00382-018-4147-x

Konstali, K., & Sorteberg, A. (2022). Why has precipitation increased in the last 120 years in Norway? *Journal of Geophysical Research: Atmospheres*, *127*(15), e2021JD036234. https://doi.org/10.1029/2021jd036234

Lavers, D. A., Villarini, G., Allan, R. P., Wood, E. F., & Wade, A. J. (2012). The detection of atmospheric rivers in atmospheric reanalyses and their links to British winter floods and the large-scale climatic circulation. *Journal of Geophysical Research*, *117*(D20), D20106. https://doi.org/10.1029/2012JD018027

Lind, P., Belušić, D., Christensen, O. B., Dobler, A., Kjellström, E., Landgren, O., et al. (2020). Benefits and added value of convection-permitting climate modeling over Fenno-Scandinavia. *Climate Dynamics*, *55*(7), 1893–1912. https://doi.org/10.1007/s00382-020-05359-3

Lind, P., Belušić, D., Médus, E., Dobler, A., Pedersen, R. A., Wang, F., et al. (2022). Climate change information over Fenno-Scandinavia produced with a convection-permitting climate model. *Climate Dynamics*, *61*(1–2), 519–541. https://doi.org/10.1007/s00382-022-06589-3

Lucas-Picher, P., Argüeso, D., Brisson, E., Tramblay, Y., Berg, P., Lemonsu, A., et al. (2021). Convection-permitting modeling with regional climate models: Latest developments and next steps. *WIREs Climate Change*, *12*(6), e731. https://doi.org/10.1002/wcc.731

Lucas-Picher, P., Brisson, E., Caillaud, C., Alias, A., Nabat, P., Lemonsu, A., et al. (2024). Evaluation of the convection-permitting regional climate model CNRM-AROME41t1 over Northwestern Europe. *Climate Dynamics*, *62*(6), 4587–4615. https://doi.org/10.1007/s00382-022-06637-y

Lussana, C., Saloranta, T., Skaugen, T., Magnusson, J., Tveito, O. E., & Andersen, J. (2018). seNorge2 daily precipitation, an observational gridded dataset over Norway from 1957 to the present day. *Earth System Science Data*, *10*(1), 235–249. https://doi.org/10.5194/essd-10-235-2018

Médus, E., Thomassen, E. D., Belušić, D., Lind, P., Berg, P., Christensen, J. H., et al. (2022). Characteristics of precipitation extremes over the Nordic region: Added value of convection-permitting modeling. *Natural Hazards and Earth System Sciences*, *22*(3), 693–711. https://doi.org/10.5194/nhess-22-693-2022

Michel, C., Sorteberg, A., Eckhardt, S., Weijenborg, C., Stohl, A., & Cassiani, M. (2021). Characterization of the atmospheric environment during extreme precipitation events associated with atmospheric rivers in Norway—Seasonal and regional aspects. *Weather and Climate Extremes*, *34*, 100370. https://doi.org/10.1016/j.wace.2021.100370

Pichelli, E., Coppola, E., Sobolowski, S., Ban, N., Giorgi, F., Stocchi, P., et al. (2021). The first multi-model ensemble of regional climate simulations at kilometer-scale resolution part 2: Historical and future simulations of precipitation. *Climate Dynamics*, *56*(11–12), 3581–3602. https://doi.org/10.1007/s00382-021-05657-4

Poujol, B., Mooney, P. A., & Sobolowski, S. P. (2021). Physical processes driving intensification of future precipitation in the mid- to high latitudes. *Environmental Research Letters*, *16*(3), 034051. https://doi.org/10.1088/1748-9326/abdd5b

Prein, A. F., Gobiet, A., Suklitsch, M., Truhetz, H., Awan, N. K., Keuler, K., & Georgievski, G. (2013). Added value of convection permitting seasonal simulations. *Climate Dynamics*, *41*(9), 2655–2677. https://doi.org/10.1007/s00382-013-1744-6

Prein, A. F., Langhans, W., Fosser, G., Ferrone, A., Ban, N., Goergen, K., et al. (2015). A review on regional convection-permitting climate modeling: Demonstrations, prospects, and challenges. *Reviews of Geophysics*, *53*(2), 323–361. https://doi.org/10.1002/2014rg000475

SURFEX. (2022). Welcome to the SURFEX home page [Software]. *SURFEX*. Retrieved from https://www.umr-cnrm.fr/surfex/

Tarasova, L., Lun, D., Merz, R., Bloschl, G., Basso, S., Bertola, M., et al. (2023). Shifts in flood generation processes exacerbate regional flood anomalies in Europe. *Communications Earth & Environment*, *4*(1), 49. https://doi.org/10.1038/s43247-023-00714-8

Utsumi, N., Seto, S., Kanae, S., Maeda, E. E., & Oki, T. (2011). Does higher surface temperature intensify extreme precipitation? *Geophysical Research Letters*, *38*(16), L16708. https://doi.org/10.1029/2011GL048426

Vanden Broucke, S., Wouters, H., Demuzere, M., & van Lipzig, N. P. M. (2019). The influence of convection-permitting regional climate modeling on future projections of extreme precipitation: Dependency on topography and timescale. *Climate Dynamics*, *52*(9), 5303–5324. https://doi.org/10.1007/s00382-018-4454-2

Vormoor, K., Lawrence, D., Heistermann, M., & Bronstert, A. (2015). Climate change impacts on the seasonality and generation processes of floods—Projections and uncertainties for catchments with mixed snowmelt/rainfall regimes. *Hydrology and Earth System Sciences*, *19*(2), 913–931. https://doi.org/10.5194/hess-19-913-2015

Wang, P., Leung, L. R., Lu, J., Song, F., & Tang, J. (2019). Extreme wet-bulb temperatures in China: The significant role of moisture. *Journal of Geophysical Research: Atmospheres*, *124*(22), 11944–11960. https://doi.org/10.1029/2019jd031477

Whan, K., Sillmann, J., Schaller, N., & Haarsma, R. (2020). Future changes in atmospheric rivers and extreme precipitation in Norway. *Climate Dynamics*, *54*(3), 2071–2084. https://doi.org/10.1007/s00382-019-05099-z

Xie, K. (2025a). Extreme_results [Dataset]. *Zenodo*. https://doi.org/10.5281/zenodo.15696381

Xie, K. (2025b). Extreme_Codes [Software]. *Zenodo*. https://doi.org/10.5281/zenodo.15696296

Xie, K., Li, L., Chen, H., Mayer, S., Dobler, A., Xu, C. Y., & Gokturk, O. M. (2025). Enhanced evaluation of hourly and daily extreme precipitation in Norway from convection-permitting models at regional and local scales. *Hydrology and Earth System Sciences*, *29*(8), 2133–2152. https://doi.org/10.5194/hess-29-2133-2025